

1 **Response type roughness measurement and cracking detection method**
2 **by using smartphone**

3 YAGI, Koichi

4 *CEO, BumpRecorder Co., Ltd., Tokyo, Japan*

5 *yagi@bumprecorder.com, Akabane 1-59-6-102, Kita-ku, Tokyo, Japan*

6

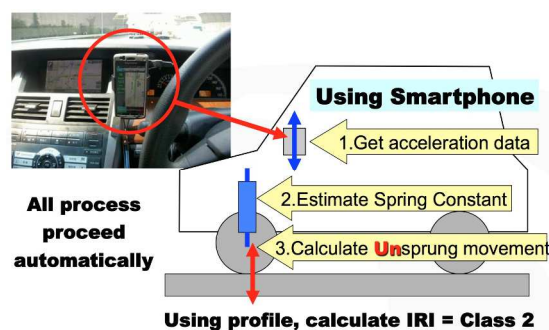
7 As for pavement maintenance management, cracking, rut and roughness are important issues. In
8 recent years, with the spread of smartphones, the new response type of the measurement method
9 has been developed, and it has been adopted as actual evaluation by local governments. In this
10 paper, at first, response type roughness measurement technology and measurement repeatability
11 will be discussed. In detail, by using developed IRI class 2 method named "BumpRecorder"
12 longitudinal profile first, then IRI by quarter car simulation can be calculated. Calculated data
13 about road roughness all over Japan has been recorded since 2011 until now, that is more than
14 1.8 million km long as of Sep. 2016. Especially road cracking is more significant issue than
15 roughness. However, previously, it was difficult to detect by the conventional method of the
16 response type. In this paper, the response type cracking detection method will be proposed. It
17 only needs a smartphone, not requiring any other devices. The detection principle and results
18 will be reported. In addition, as for roughness and cracking evaluation, section determination is
19 important. Traditionally, a kilo post marker has been used for section determination. But it
20 requires long time and much cost to make kilo post data. To solve such problems in this paper,
21 "Square Mesh Section" will be proposed. It is determined by latitude and longitude. Using this
22 section, only by collecting GPS data, it will be determined the same section under repeated
23 measurement. Response type roughness measurement and cracking detection and Square Mesh
24 Section will reduce data collection and analysis costs for pavement maintenance management.
25
26 Keywords: response type measurement, roughness measurement, cracking detection,
27 smartphone

28 1 Response type roughness measurement

29 For roughness measurement, the smartphone measurement technology has been
30 developed. It measures vehicle vibration by using smartphone built-in accelerometer
31 and GPS. Then road roughness e.g. IRI can be calculated. This convenient method
32 brings routinely inspection and screening. "BumpRecorder" is one of the applications.
33 In this paper, measurement principle is explained as follows.

34 A smartphone is placed on the vehicle dashboard which is located over the vehicle
35 suspension. In the case of this response type measurement, because a vehicle has
36 suspensions, recording acceleration is easily influenced by a vehicle model and its
37 driving speed. As the result, measurement results are not stable. To improve this
38 problem, calibration driving has been applied for each vehicle before measurement
39 driving. The biggest expectancy of the response type measurement is its convenience.
40 However, calibration driving decreases its advantage. And traditional response type
41 measurement needs correlation formula which is determined experimentally during
42 calibration driving. It means that traditional response type IRI measurement is IRI class
43 3. This method is not only inconvenient but also inaccurate in actual road conditions
44 where are not including situations at calibration driving roads.

45 "BumpRecorder" is not requiring calibration driving. It is IRI class 2, which is
46 increasing measurement convenience and measurement repeatability. In order to get
47 these features, vibration frequency analysis is applied. Figure 1 is drawing the
48 calculation steps.



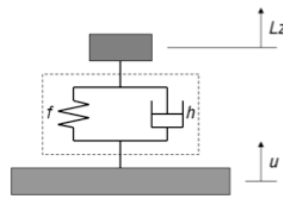
49

50 Figure 1. Roughness calculation steps

51 At first, by using FFT, vehicle suspensions resonant frequency and damping ratio are
52 estimated. Even if recorded acceleration is including several resonant frequencies,

53 suspensions movement is a main vibration, so its resonant frequency can be found
 54 around 1.5[Hz] easily.

55 Next, by using this spring parameters, the equation of motion of the one mass spring
 56 model is calculated. This model is drawn in Figure 2. An equation (1) is an equation of
 57 motion for this model. In this equation, Lz is a sprung vertical movement, " u " is an
 58 unsprung vertical movement, " ω " is an angular frequency, " h " is a damping ratio. " ω " is
 59 defined by equation (2). In this equation, " f " is a resonant frequency. Here, previous
 60 FFT result is using for " h " and " f ".



61

62 Figure 2. One mass spring model

63
$$\ddot{Lz} + 2h\omega(\dot{Lz} - \dot{u}) + \omega^2(Lz - u) = 0 \quad (1)$$

64
$$\omega = 2\pi f \quad (2)$$

65 And finally, an unsprung movement " u " is assumed that it is equal to road longitudinal
 66 profile, and it is calculating the Quarter Car simulation, then IRI will be calculated.

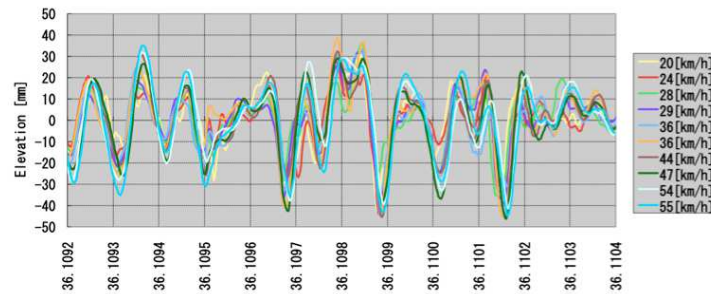
67

68 2 Experimental results

69 Figure 3 shows the sprung elevation of each position calculated by double integral of
 70 sprung vertical acceleration. In this experiment, TOYOTA PRIUS is used, which has
 71 2,700 [mm] wheelbase and 1,400 [kg] weight, driven at several speed from 20[km/h] to
 72 55[km/h]. Look at the period from latitude 36.1095 to 36.1096, and the period from
 73 latitude 36.1098 to 36.1099, the sprung elevation profile of each speed is different.

74 Figure 4 shows unsprung elevation of each position calculated by equation (1). Look at
 75 the two periods above. Difference of unsprung elevation for each speed is smaller than
 76 sprung elevation. It means that unsprung elevation estimation is effective to get good

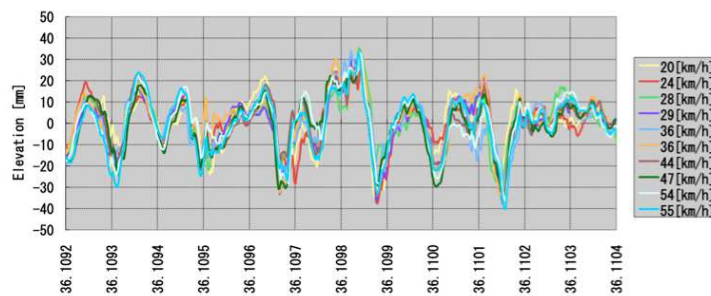
77 repeatability. And unsprung elevation can reproduce more pointed profile than sprung
78 elevation profile. It means that unsprung elevation estimation provides higher response,
79 and a vehicle can be driven at faster speed with higher accuracy. This result says this
80 method could reduce time and costs for the roughness measurement.



81

82

Figure 3. Sprung elevation profile.

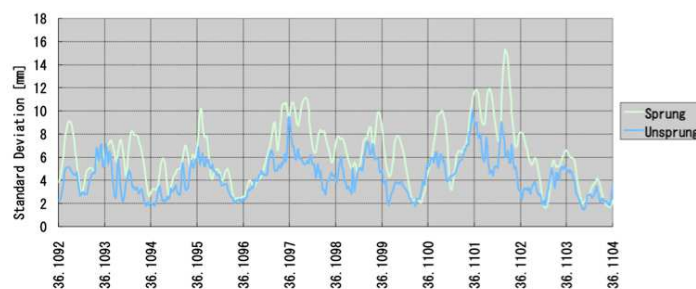


83

84

Figure 4. Unsprung elevation profile.

85 To compare dispersion of the measurement sprung elevation with the estimated
86 unsprung elevation, elevation standard deviations of each speed are calculated at each
87 position. This value is drawn in Figure 5. It clearly shows unsprung standard deviation
88 is smaller than sprung standard deviation. Look at position around latitude 36.11017.
89 The standard deviation of sprung elevation is 15[mm], and unsprung elevation is 6[mm].
90 Unsprung elevation dispersion is reduced to 40% variability.



91

92 Figure 5. Elevation standard deviation.

93

94 **3 Response type cracking detection**

95 Response type cracking detection method is described. Target cracking is an alligator
96 cracking like Figure 6. An alligator pattern size is about 20~40 [cm]. To detect this
97 cracking, smartphone built-in accelerometer and GPS are only used, any other sensors
98 not required. The smartphone is placed on the vehicle dashboard. These measurement
99 conditions are the same as the response type roughness measurement. It means that
100 roughness measurement and cracking detection can be done by the same smartphone at
101 the same time.



102

103 Figure 6. Target cracking of alligator cracking

104 When the vehicle is passing over road cracking, the vehicle will vibrate. For example, a
105 vehicle speed is 36 [km/h] or 10 [m/s], and an accelerometer sampling cycle is 100 [Hz],
106 the vehicle is driven 10 [cm] in one sampling cycle. It means that the size of each
107 cracking is about few sampling cycles. An expecting acceleration frequency is
108 approximately 30 [Hz] to 50 [Hz]. This frequency is higher than vehicle natural
109 frequency of the suspension's 1.5 [Hz] and tire's 15 [Hz].

110 To detect amplitudes of each frequency, FFT calculation is used. This time, the data size
111 of FFT is using about 1 cycle of suspension's natural frequency, which is about 0.7 [s].
112 For FFT, the number of samples must be power of 2. So, the number of data sample is
113 selected by the biggest number of power of 2 less than the sampling cycle number. For
114 example, when the sampling cycle is 100 [Hz], the number of FFT sample is 64.

115

116 4 Basic experimental results

117 For the test drive, TOYOTA PRIUS was used. And 3 models of smartphone were used.
118 One is Sony Xperia Z1 which has 200 [Hz] sampling cycle, another one is Sharp
119 AQUOS Phone SH-12C which has 100 [Hz], and the other is HTC EVO 4G which has
120 50 [Hz]. This experimental driving was done in Tokyo, Japan. Figure 7 shows IRI
121 conditions in this road. Line colour indicates IRI value. Light blue is indicating smooth
122 road, blue, green, brown are rougher road, and red is the roughest road. In this
123 experiment, the start point is light blue circle position, and the end point is orange circle
124 position in Figure 7.

125 FFT result is drawn in Figure 8. The horizontal axis is the longitude [deg.] of driving
126 path. The starting point shows located at right hand side. The vertical axis shows FFT
127 frequency [Hz]. And the circle diameter indicates the wave strength for each frequency
128 of each position. In Figure 8, for example, the longitude around 139.71702 has cracking.
129 In this point, FFT frequency around 50[Hz] has the large strength. As above paragraph
130 of this paper indicates, cracking features are expecting around 30~50[Hz]. The result of
131 Figure 8 is matched with this expecting.

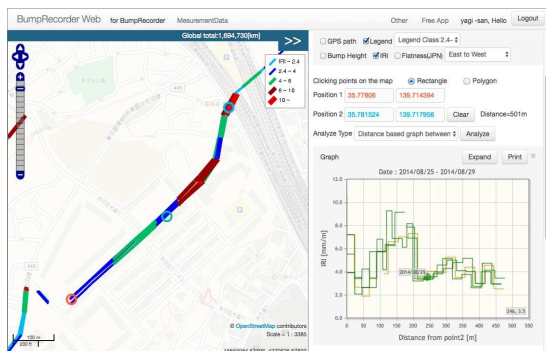


Figure 7. IRI conditions

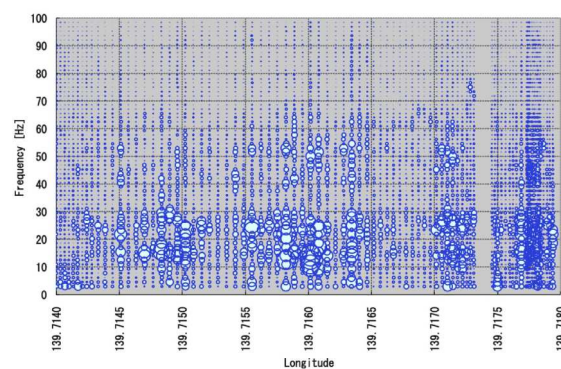


Figure 8. FFT result

132 5 Cracking detecting logic and experiment on actual road conditions

133 As above experiment, the cracking detection logic is designed as follows. For FFT
134 analysis data, frequency is defined $f(i)$, and amplitude is defined $a(i)$. The weighted
135 average of frequency f_{ave} is defined by equation (3). And mean amplitude is defined a_{ave} .
136 Here, the cracking index CI is defined by equation (4). When there is cracking, CI is
137 expected to become large value.

138
$$f_{ave} = \frac{\sum_i f(i) \times a(i)}{\sum_i a(i)} \quad (3)$$

139
$$CI = f_{ave} \times a_{ave} \quad (4)$$

140 Figure 9 shows cracking index CI recorded by Sony Xperia Z1, which has 200[Hz]
 141 sampling cycle. In this figure, the horizontal axis is longitude, the vertical axis is
 142 latitude, and the circle diameter indicates CI value. Especially, the red circle indicates
 143 the large CI point that is estimated cracking point. Position 1 has cracking and CI
 144 becomes large. It means cracking is detected successfully. Position 2 is CI becomes
 145 large. But here has no cracking. This road is paved by concrete. Figure 10 shows picture
 146 of this road. Aggregate is seen on the concrete surface., therefore road surface is uneven.
 147 As the result, cracking index CI is reflecting this concrete road.

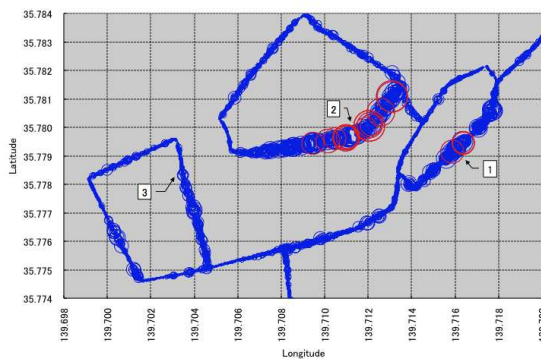
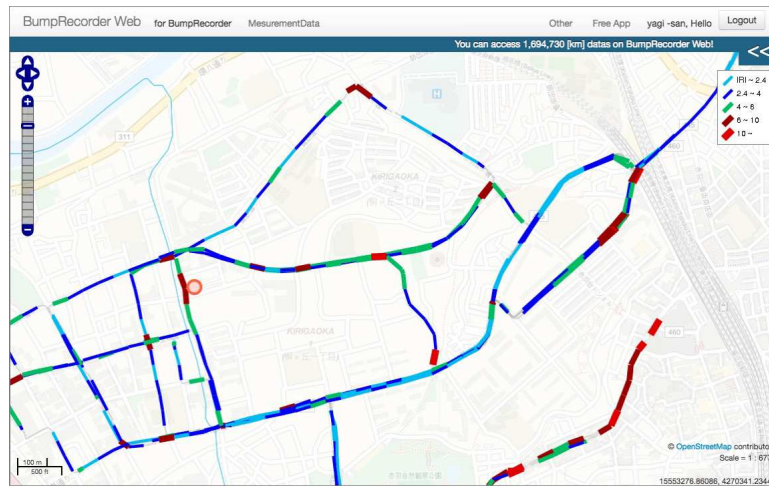


Figure 9. CI by 200 [Hz] sampling cycle

Figure 10. Concrete road at position 2

148 Figure 11 shows IRI conditions of experimental road. An orange circle position of
 149 Figure 11 is the point 3 of Figure 9. Look at Figure 11, this position's roughness is
 150 serious. But there is no cracking. Look at Figure 9, CI is not large. According to this
 151 result, CI is reflecting cracking, not reflecting roughness. That is good characteristic.

152 Figure 12 shows the cracking index CI which is recorded by Sharp AQUOS Phone SH-
 153 12C, which has 100 [Hz] sampling cycle. Figure 13 is recorded by HTC EVO 4G which
 154 has 50 [Hz]. These figures clearly show the detecting trend is same. According to this
 155 result, cracking index CI can be used for cracking detections for several types of
 156 smartphones.



157

158

Figure 11. IRI conditions

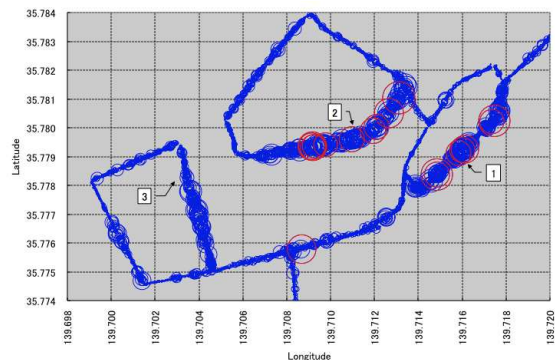
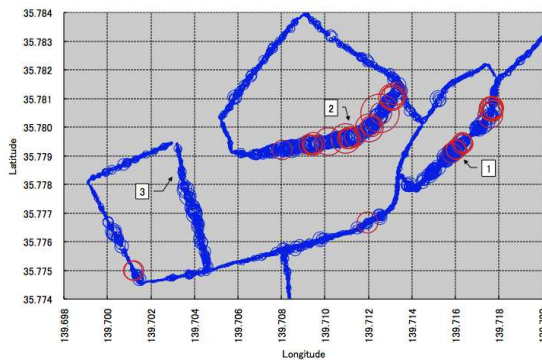


Figure 12. CI by 100 [Hz] sampling cycle

Figure 13. CI by 50 [Hz] sampling cycle

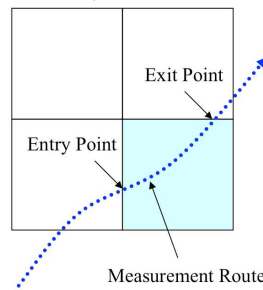
159

160 6 "Square Mesh Section" for section determination

161 To calculate IRI, a calculating section is an important factor. Traditionally, this section
162 has been defined by road location markers e.g. kilo-post data. Kilo-post data is prepared
163 for main roads, but not for community roads. For this reason, the data has not been
164 easily defined on the community road, which makes roughness measurement difficult. It
165 means that kilo-post data was not easily defined on the community road, which makes
166 roughness measurement difficult. When kilo-post data is not used, GPS data is
167 separated in a certain distance, for example each 100[m]. This calculation is easy. But
168 unfortunately GPS data has an error. So, even if origin position is adjusted, a section
169 separating point could be deviated, and this deviation is increase, depending on the

170 length of measurement distance. In this situation, when needed the comparison of the
 171 current IRI with the previous one, because IRI section is not same, a comparison check
 172 becomes difficult.

173 To improve this situation, "Square Mesh Section" is proposed. It can pick up the same
 174 section at anytime, anywhere, only by using GPS data. Square shape mesh is defined by
 175 the longitude and the latitude on the earth. When the driving path is crossing over this
 176 mesh, IRI section is determined from an entry point to an exit point. Figure 14 shows
 177 "Square Mesh Section".



178

Figure 14. "Square Mesh Section" for IRI calculation section

179
 180 In detail, for this Square Mesh, East West width is defined by $1/8192=2^{-13}$ length for
 181 each 1 degree of the longitude. It is about 10[m] around Japan located at latitude 35
 182 degrees. And North South width is defined by the same length of East West width. For
 183 this square shape mesh, "Square Mesh Code" is defined by a pair code for the longitude
 184 and the latitude. An equation (5) defines *LonCode* for the longitude code, and an
 185 equation (6) defines *LatCode* for latitude code. *LonCode* and *LatCode* are integer.

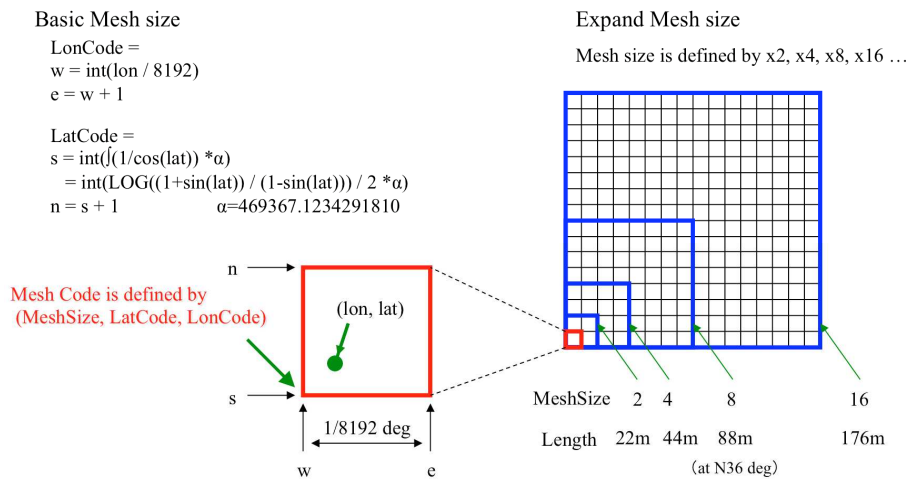
186
$$LonCode = \text{int}\left(\frac{longitude}{2^{13}}\right) \quad (5)$$

187
$$LatCode = \text{int}\left(\int \frac{1}{\cos(latitude)} \times \alpha\right) = \text{int}\left(\log \frac{1 + \sin(latitude)}{1 - \sin(latitude)} \times \frac{\alpha}{2}\right) \quad (6)$$

188 Here, " α " is defined by *LatCode* is 1 when *LonCode* is 1. That is as follows.

189
$$\alpha = 469,367.1234 \quad (7)$$

190 In addition, a magnification mesh is defined to use longer section for IRI calculation. A
 191 magnification mesh is defined by 2 times, 4 times, 8 times, and 16 times width of
 192 original mesh width. As the result, "Square Mesh code" is defined by array of
 193 (*MeshSize, LatCode, LonCode*). It shows in Figure 15.



194

195

Figure 15. Definition of the "Square Mesh Code"

196

197 6 Conclusions

198 In this paper, the response type roughness measurement method and the cracking
 199 detection method are proposed. Both of them are using the same acceleration data and
 200 GPS data which are recorded at same time by same device. And the proposed roughness
 201 measurement "BumpRecorder" is calculating longitudinal profile first and then IRI is
 202 calculated by Quarter Car Simulation. That is IRI class 2. In Addition, "Square Mesh
 203 Section" is proposed for IRI calculation section. It is defined by latitude and longitude.
 204 It is not requiring kilo-post data. "BumpRecorder" and "Square Mesh Section" is
 205 reducing measurement costs and lead-time. For these reasons, the methods enable users
 206 to operate routine measurement. Routine measurement is available with these methods,
 207 and it will bring an increase in level of pavement maintenance management.

208

209 References

210 Michael Nieminen, et.al, Improving Automated Distress Rating Using Two- and Three-
 211 Dimensional Data Concurrently, Transportation Research Board 93rd Annual Meeting,
 212 14- 6653, 2014

- 213 TOMIYAMA Kazuya, et.al, Lifting Wavelet Transform for Distress Identification
214 Using Response-Type Profilers, Transportation Research Board 93rd Annual Meeting,
215 14-3520, 2014
216 YAGI Koichi, Road Bump Detection Method by Using Smartphone and Measurement
217 Result on TOHOKU Earthquake, The 11th ITS AP Forum 2011 Kaohsiung, CD-ROM,
218 2011